Electronic supplementary information

Selective and sensitive determination of hydroxyl radicals generated from living cells through electrochemical impedance method

*Anwei Zhu, Yan Liu, Qi Rui, Yang Tian**

Department of Chemistry, Tongji University, Siping Road 1239, Shanghai 200092, People's Republic of China

1. Experimental section

Reagents and Materials. Indium tin oxide (ITO)-coated glass plates with a square resistance of 10–20 Ω cm^{-2} were obtained from Nanbo (Shenzhen, China). Anatase TiO_2 (STS-21) was obtained from Ishihara Sangyo Kaisha. Hydrogen tetrachloroaurate (III) trihydrate ($HAuCl_4 \cdot 3H_2O$, 99.99%), homovanillic acid (3-methoxy-4-hydroxyphenylacetic acid, HVA), horse radish peroxidase (POD), 2,2-Azobis (2-amidinopropane) dihydrochloride (AAPH) and Lipopolysaccharide (LPS) purified from Salmonella typhimurium were purchased from Aldrich. 1-Octadecanethiol (ODT) and sodium molybdenum oxide dihydrate were obtained from Alfa Aesar. Peroxynitrite was purchased from R&D Systems. Hanks' balanced salt solution (HBSS) was bought from GIBCO. Ceric sulfate was obtained from Sinopharm Chemical Reagent Co., Ltd. (China). All other reagents were of analytical grade and used as received. All aqueous solutions were prepared with Milli-Q water and were deaerated with high purity nitrogen before experiments. In selectivity test, O_2^- was chemically generated by the reaction between H_2O_2 (10 mM) and cerium sulfate ($Ce(SO_4)_2$) (100 mM)).[S1] Singlet oxygen ($^1O_2$) was generated as a product of the disproportionation of H_2O_2 (20 mM) in alkaline solution (pH=10) catalyzed by molybdate ions (20 mM).[S2] Alkyl peroxyl radical ($ROO^{\cdot}$) was generated by thermolysis of AAPH (10 mM) in air-saturated aqueous solution at 310 K.[S3] Peroxynitrite ($ONOO^-$) (10 mM) was generated by diluting commercially available peroxynitrite solution with a strongly basic solution (0.1 M NaOH). $HO^{\cdot}$ was generated by the Fenton reaction (0.1 mM H_2O_2 and 0.6 mM Fe^{II}(EDTA)). Their influences on the charge transfer resistance (R_{ct}) of redox probe at the ODT-modified gold film were all obtained after 20 min reaction time.

Preparation and Modification. Gold flower-like nanostructures were electrodeposited onto an indium tin oxide (ITO)-coated glass plate at −0.08 V versus Ag|AgCl (in saturated KCl) for 5 min from 40 mM $HAuCl_4$ solution. The ODT SAM was fabricated by immersing the gold film in an absolute ethanol solution containing 1 mM ODT for 7–12 h. A TiO_2 film was prepared as follows: an ITO-coated glass plate was covered with anatase TiO_2 sol by spin-coating method and then sintered at 723 K for 60 min.

Apparatus and Measurements. Scanning electron microscopy (SEM) images were taken by a Quanta 200 FEG (FEI Company). X-ray diffraction (XRD) measurements were carried out via a BRUKER D8 diffractometer (40 mA / 40 kV), using Cu $K\alpha_1$ radiation (λ = 1.54 Å) over the 2θ range of 10° to 70°. X-ray photoelectron spectroscopy (XPS) (Model PHI 5000) was used to track the modification and decomposition of ODT. The water contact angle was measured with a contact angle meter (Model JC 2000A, Shanghai, China). Fluorescence spectrum was determined with a Perkin-Elmer LS-55 spectrophotometer, in which excitation and emission slits were all 5 nm. Electrochemical measurements were carried out by a computer-controlled CHI 660D electrochemical workstation (Shanghai, China) in a home-made three-electrode electrochemical cell using a KCl-saturated Ag|AgCl electrode as reference electrode and a platinum wire as auxiliary electrode. All electrochemical impedance spectroscopy (EIS) experiments were performed in 0.1 M KCl solution containing equimolar (0.01 M) $[Fe(CN)_6]^{3-/4-}$, and the experimental conditions were as follows: potential, 0.290 V (the formal potential of the $[Fe(CN)_6]^{3-/4-}$ couple); alternative voltage, 5 mV; frequency range, $0.1–10^5$ Hz. As more and more pinholes and/or larger pinholes were generated in the process of $HO^{\cdot}$-stimulated oxidation and decomposition of alkyl monolayer, it facilitated the solvent/ion permeation into the bulk of SAM. As expected, the slope of the low-frequency region observed in the Nyquist plots for the ODT-modified gold flower-like nanostructures in our system was not unity. Moreover, in the absence of redox probe – $Fe(CN)_6^{3-/4-}$, the obtained non-Faradaic impedance consisted of an interfacial resistance in parallel with the double layer capacitance. This resistance due to the movement of ions in and out the SAM film is quite separate from the charge transfer resistance, which represents the flow of charge across the modified interface into the electrode.[S4] Thus, it is reasonable to include the SAM resistance as a parallel component to the charge transfer resistance of the redox couple in solution and the equivalent circuit is therefore shown as Fig. S1. It should be noted that the Randles circuit model will fit better only when the ODT-covered electrode was nearly completely decomposed by $HO^{\cdot}$ with a unite slope of the low-frequency region in the Nyquist plots.

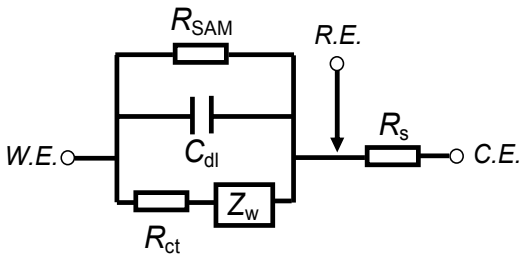

Fig. S1 Equivalent circuit model used to obtain equations for Z_{re} and $-Z_{im}$ in our system.

Fig. S1 shows a schematic diagram for the ideal circuit used to describe the observations in this study. It consists of the resistance of electrolyte (R_s), the charge-transfer resistance (R_{ct}), the impedance due to mass transfer (Z_w), the double layer capacitance (C_{dl}) and the parallel interfacial resistance R_{SAM} due to ions flowing in the region of SAM. A model[S5] based on the work of Matsuda[S6] and Amatore[S7] was developed to fit the Faradaic impedance data for charge-transfer reactions at perforated SAM-coated electrodes. The expressions for the Faradaic impedance of a microporous SAM in the limit of high frequency are

$$Z_{re}(\omega) = R_{ct} / (1 - \theta) + \sigma / \omega^{1/2} + \sigma / [(1 - \theta)\, \omega^{1/2}] \quad (1)$$

$$Z_{im}(\omega) = \sigma / \omega^{1/2} + \sigma / [(1 - \theta)\, \omega^{1/2}] \quad (2)$$

The equivalent expressions for the low frequency case are

$$Z_{re} = R_{ct} / (1 - \theta) + \sigma / \omega^{1/2} + [\sigma r_a (0.72D)^{1/2} / (1 - \theta)] \quad (3)$$

$$Z_{im} = \sigma / \omega^{1/2} \quad (4)$$

Z_{re} and Z_{im} are the real and imaginary impedances respectively, σ is the Warburg impedance slope, ω is the radial frequency ($2\pi f$), r_a is the radius of the pore, D is the diffusion coefficient, and θ is the degree of coverage. All of the useful information about the SAM-coated electrode can be obtained from a graph of Z_{re} vs $\omega^{-1/2}$ if the impedance of the electrode can be measured over a sufficiently wide frequency range.

From the equivalent circuit it is possible to write down algebraic equations for the $-Z_{im}$ and Z_{re} and fit the experimental data, in the complex plane, to obtain the magnitude of the ideal circuit element. By using

an algorithm based on that of Macdonald,[S8] both $-Z_{im}$ and Z_{re} data were used in the impedance fit (at the same time) by complex nonlinear regression (CNLS).[S9] Fig. S2 shows the results of impedance spectroscopy on the gold flower-like nanostructures modified with ODT after being attacked by $HO^{\cdot}$ in the remote TiO_2 photocatalytic oxidation system for 30 min and 300 min, respectively. It is clear that the slope of the low-frequency region for both reaction times are not unity and the CNLS regression analysis based on the selected model rather than the Randles circuit fit the experiment data better.

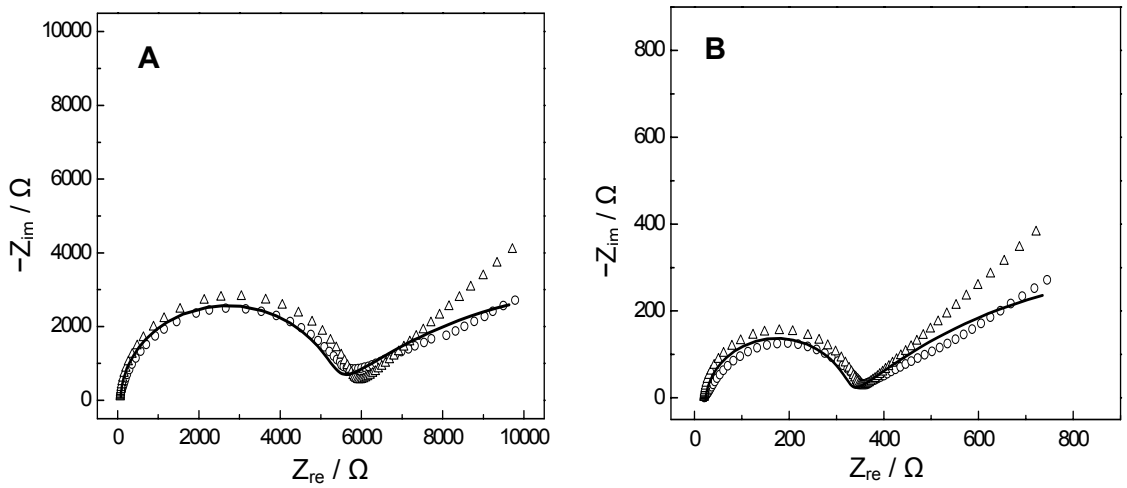

Fig. S2 Nyquist plots obtained at the gold flower-like nanostructures modified with ODT after being attacked by $HO^{\cdot}$ in the remote TiO_2 photocatalytic oxidation system for (A) 30 min and (B) 300 min in 0.1 M KCl solution containing 0.01 M $[Fe(CN)_6]^{3-/4-}$.The electrode potential was 0.290 V: (o) experimental data; (Δ) the best CNLS regression to the Randles circuit model; (–) fit to the selected model using CNLS regression.

Cell Culture. Mononuclear macrophage cells RAW264.7 were obtained from Baili Biotechnology company (Shanghai, China). Cell culture media and supplements were purchased from Invitrogen (Carlsbad, USA). The cells were cultured at 310 K under a humidified 5% CO_2 atmosphere in Dulbecco's Modified Eagle's medium (DMEM) supplemented with 10% fetal bovine serum, 100 units mL^{-1} penicillin and 100 μg mL^{-1} streptomycin.

2. SEM image of gold flower-like film.

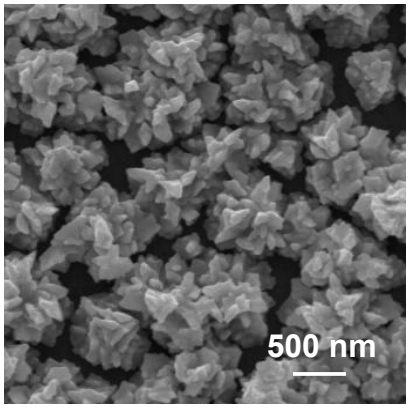

Fig. S3 SEM image of gold flower-like film.

3. Optimized conditions

Intensity of irradiated UV light. As shown in Fig. S4, the irradiation time required to completely remove the SAM of ODT extends from about 0.5 h to 6.5 h at different intensities of UV light. In order to acquire a wider detection linear range and a lower detectable concentration of H_2O_2, the intensity of UV light was chosen to be 7.6 mW cm^{-2}.

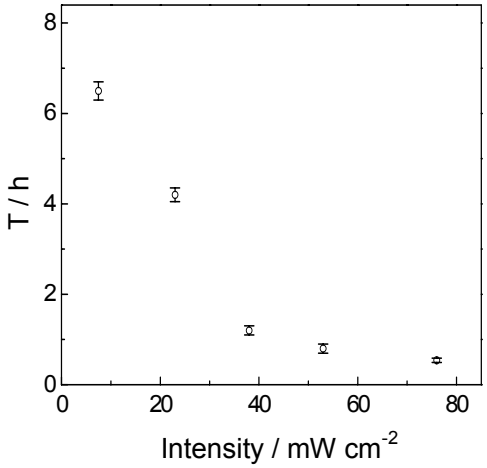

Fig. S4 The irradiation time required for the completely removal of ODT SAM versus the intensity of UV light. The error bars were obtained from three independent experiments for each UV light intensity.

Surface area of ODT-modified gold film. As shown in Fig. S5, the charge-transfer resistance (R_{ct}) of $[Fe(CN)_6]^{3-/4-}$ increased to a certain extent with the surface area of ODT-modified gold film. In order to

obtain a larger ΔR_{ct} or a broader dynamic linear range, the surface area was ultimately chosen to be 1×1 cm^2 by taking into account of the restriction on the area of light source.

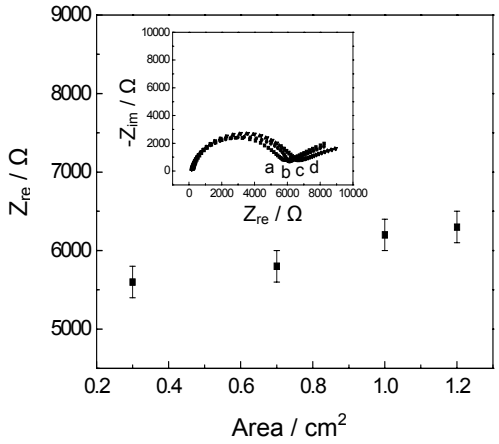

Fig. S5 Plot of R_{ct} versus the area of ODT-modified gold films. Inset: Nyquist plots obtained at ODT-modified gold film in 0.1 M KCl solution containing 0.01 M $[Fe(CN)_6]^{3-/4-}$. The surface area of the electrode: (a) 0.3 cm^2, (b) 0.7 cm^2, (c) 1.0 cm^2, (d) 1.2 cm^2. The error bars were obtained from five independent experiments for each area.

Thickness of TiO_2 film. As shown in Fig. S6, the photocatalytic activity was enhanced with the increasing thickness of TiO_2 film up to ~3 μm. Since the transmittance of TiO_2 film decreased with the increasing of film thickness, no increase in the photocatalytic activity of TiO_2 film was observed when the TiO_2 film with the thickness of more than ~3 μm was employed. Thus, we optimized the thickness of TiO_2 film to be ~3 μm.

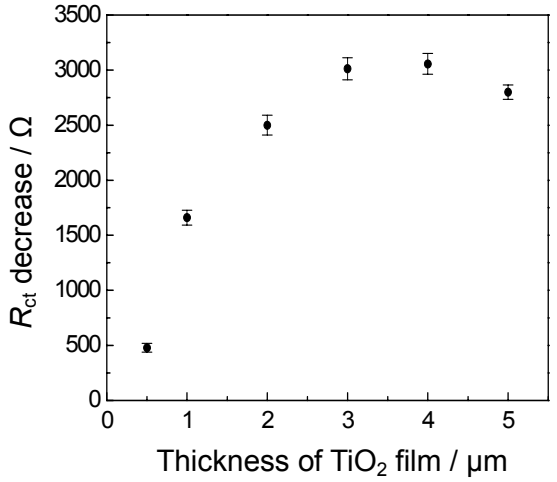

Fig. S6 Effect of the thickness of TiO_2 film on the R_{ct} decrease obtained at SAM-modified gold flower-like film. Apparent area of TiO_2 film: 1 cm^2; relative humidity: 60%; irradiation time: 3 h.

Distance between TiO_2 film and ODT-modified substrate. To optimize the distance between TiO_2 film and ODT-modified substrate, we referenced the work of Tatsuma's group.[S10] Although the remote oxidation could take place at distance up to 2.2 mm, the response time for removal of organic probes increased with the increasing distance between TiO_2 film and ODT-modified electrode from 50 μm to 2.2 mm. Thus, we performed the experiments with the gap of ~50 μm.

4. Determination of H_2O_2 Released from TiO_2 to Air.

A home-made flow-throw cell was prepared as Scheme S1. A TiO_2-coated ITO glass plate and a bare glass plate faced to each other with a small intervening gap (~50 μm), and the sides were sealed with glass plates and silicone except for inlet and outlet tubes. The TiO_2 side was exposed to UV light (7.6 mW cm^{-2}) with a cold mirror filter attached. The purified air passed through the photocatalyst cell (2 mL/min) and the out-flowing gas from the irradiated cell was flushed through a 3 ml optimized collecting solution containing 0.1 M tris buffer (pH 8.50), 2.5 mM homovanillic acid (3-methoxy-4-hydroxyphenylacetic acid, HVA), and 2.0 U ml^{-1} horse radish peroxidase (POD) for a reaction time of 30 min at 298 K. The HVA oxidation product was determined by fluorescence spectrometer to measure the amount of H_2O_2. The fluorescence of the collecting solution was recorded at a λ_{ex} of 313 nm and a λ_{em} of 425 nm. The relative humidity was 60%, and the room temperature was 298 K, unless otherwise noted.

Scheme S1. Schematic illustration of the experimental device for the detection of H_2O_2 released from TiO_2 to air.

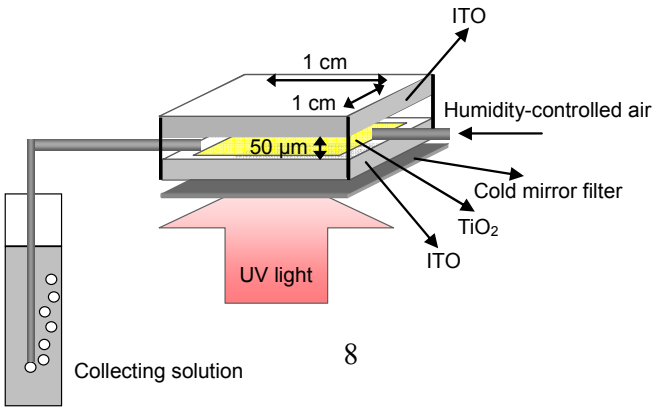

5. Control experiments

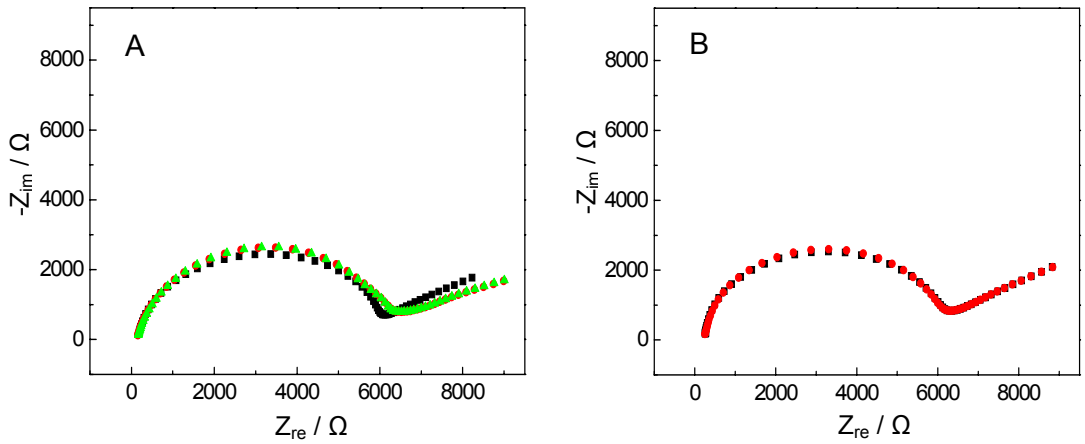

Fig. S7 (A) Nyquist plots obtained at ODT-modified gold film (red), ODT-modified gold film exposed to UV light (7.6 mW cm^{-2}) for 2 h without facing to TiO_2 film (green), and ODT-modified gold film exposed to 10 mM H_2O_2 solution for 60 min (black). (B) Nyquist plots obtained at ODT-modified gold film before (black) and after (red) being immersed in 0.1 M KCl solution containing 0.01 M $[Fe(CN)_6]^{3-/4-}$ for 20 min. All experiments were performed in 0.1 M KCl solution containing 0.01 M $[Fe(CN)_6]^{3-/4-}$.

From these control experiments, it is clear that neither UV light irradiation nor H_2O_2 can attack the SAM of ODT. The redox couple was also shown no influence on the SAM of ODT.

6. Experimental Device for Biological HO˙ Detection

Scheme S2. Schematic illustration of the experimental device for the detection of HO˙ from stimulated macrophages.

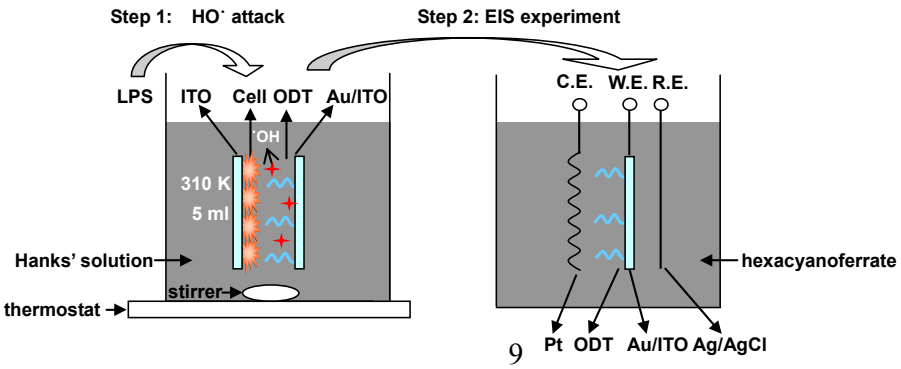

References

[S1] T. Tatsuma, S. Tachibana and A. Fujishima, *J. Phys. Chem. B*, 2001, **105**, 6987.

[S2] J. M. Aubry and B. Cazin, *Inorg. Chem.*, 1988, **27**, 2013.

[S3] H. Loertzer, S. Bauer, W. Moerke, P. Fornara and H. J. Broemme, *Transplant. Proc.*, 2006, **38**, 674.

[S4] R. P. Janek and W. R. Fawcett, *Langmuir*, 1998, **14**, 3011.

[S5] H. O. Finklea, D. A. Snider and J. Fedyk, *Langmuir*, 1993, **9**, 3660.

[S6] K. Tokuda, T. Gueshi and H. Matsuda, *J. Electroanal. Chem.*, 1979, **102**, 41.

[S7] C. Amatore, J. M. Saveant and D. J. Tessler, *J. Electroanal. Chem.*, 1983, **147**, 39.

[S8] J. R. Macdonald, Ed.; *Impedance Spectroscopy: Emphasizing Solid Materials and Systems*; John Wiley & Sons: New York, 1987.

[S9] W. T. Vetterling, B. P. Flannery, W. H. Press and S. A. Teukolsky, Numerical Recipes in C, 2nd ed. Cambridge University Press: New York, 1992; 656.

[S10] T. Tatsuma, S. Tachibana, T. Miwa, D. A. Tryk and A. Fujishima, *J. Phys. Chem. B*, 1999, **103**, 8033.